Capacitive Power Transfer System With Double T-Type Resonant Network for Mobile Devices Charging/Supply

Zhe Liu, Yu-Gang Su, *Member, IEEE*, Yu-Ming Zhao, Aiguo Patrick Hu, *Senior Member, IEEE*, and Xin Dai, *Member, IEEE*

***Abstract*—In the applications of wireless power transfer for mobile devices, the pick-up of the wireless power transfer system often needs to be moved in and moved out. A sudden change in the system structure will cause high transient voltages or currents, which could damage the power electronic device of the capacitive power transfer (CPT). In addition, the standby power of the system will be too high to work after removing the pick-up. A CPT system with double T-type resonant networks has been proposed to address these problems. The steady-state models of the system without the pick-up and normal state conditions of it are established. The relationships between the resonant network parameters are analyzed, and a systematic circuit parameter design method is provided. The proposed CPT topology and the parameter design method have been verified by simulation and experiment. The system not only achieved self-protection under severe load change but also entered standby mode automatically after the pick-up was moved out. Besides, the system is restored to the normal state condition when the pick-up is moved in without additional detection and control circuitry.**

***Index Terms*—Capacitive power transfer (CPT), double T-type resonant network, mobile device, wireless power transfer (WPT).**

I. Introduction

WIRELESS power transfer (WPT) technology utilizes a magnetic field, electric field, laser, microwave, and another medium to deliver electric power from the power source to electrical equipment without direct electrical contacts [1]–[3]. It eliminates the need for a direct conductor connection and has the advantages of convenience, flexibility, safety, and reliability [4]–[6]. With the increasing demand for wireless power supplies, it has attracted the broad attention of researchers in the world.

To realize WPT, there are two most pervasive methods, the inductive power transfer (IPT) and the capacitive power transfer (CPT). The IPT technology has developed for many years with lots of research achievements [7]–[10]. Compared with IPT, CPT is a relatively new WPT technology based on electric field coupling [11]–[13]. It provides advantageous features, such as light, thin, low-cost coupling structures, flexibility in coupling structure design, the ability to transfer power across metal barriers, and low eddy-current losses in the surrounding metallic objects [14]–[17]. CPT technology has been investigated in many fields with a wide range of power levels from several milliwatts to kilowatts. It has been applied both in low-power applications such as implanted biomedical devices, consumer electronics [18], [19] and in high-power applications such as electric vehicles charging [20]–[22].

In the application of the CPT technology, such as charging for portable electronic devices (e.g., mobile phone, iPad, laptop) and unmanned aerial vehicle, or supply for kitchen and household appliances, the pick-up of the CPT system (i.e., the load, the secondary side coupling plates, and the power conditioner circuit) often needs to be moved in and moved out. In this process, over-voltage and over-current are not allowed. Once the current and voltage of the primary inverter of the system vary dramatically, the high transient process associated may damage the semiconductor switches. Meanwhile, ideally, the system should work in standby mode automatically after the pick-up is removed for economical and reliable operation, which makes the system consume little power after the pick-up is removed. And the system restores to deliver the required power to the load effectively when the pick-up is moved in.

There were few relevant studies nowadays focused on the above problems. The conventional series inductor compensation method for CPT systems is simple and popular [13], [14]. But the inductor current will be interrupted when the branch circuit of the inductor is open suddenly, so the high voltage spikes will occur when the pick-up is removed, which can cause undesirable transient and electrical hazards. A CPT system based on a Z-impedance compensation network is proposed to address the high voltage spikes issue related to the compensation inductor

Manuscript received December 14, 2020; revised March 15, 2021 and May 27, 2021; accepted August 12, 2021. Date of publication August 18, 2021; date of current version October 15, 2021. This work was supported by the National Natural Science Foundation of China under Grant 51977015. Recommended for publication by Associate Editor R. Zane. *(Corresponding author: Yu-Gang Su.)*

Zhe Liu is with the College of Automation, Chongqing University, Chongqing 400044, China (e-mail: 809632730@qq.com).

Yu-Gang Su and Xin Dai are with the College of Automation, Chongqing University, Chongqing 400044, China, and also with the Key Laboratory of Complex System Safety and Control, Ministry of Education (Chongqing University), Chongqing 400044, China (e-mail: su7558@qq.com; toybear@vip.sina.com).

Yu-Ming Zhao is with the Chongqing Qianwei Technologies Co. LTD, Chongqing 401121, China (e-mail: 1551480934@qq.com).

Aiguo Patrick Hu is with the Department of Electrical and Computer Engineering, University of Auckland, Auckland 1142, New Zealand (e-mail: a.hu@auckland.ac.nz).

Color versions of one or more figures in this article are available at https://doi.org/10.1109/TPEL.2021.3105406.

Digital Object Identifier 10.1109/TPEL.2021.3105406

[23]. However, the current of the inverter increases dramatically after the sudden removal of secondary plates due to the input impedance decreases sharply, existing the risk of destroying the semiconductor switches of the inverter.

Although some CPT systems do not use the series inductor compensation [20], [22], these systems consume much power (high no-load losses) after the pick-up is removed, which cannot automatically enter standby mode if there is no additional detection and control circuit. Besides, these compensation topologies require extra reactive components on the secondary side, which will increase the volume and weight of the pick-up, especially in mobile devices application. In this case, the CPT system must be designed to eliminate the impact voltage and current to protect the circuit when the pick-up is removed.

To solve the above problems, add the current detection module to protect the circuit is an effective solution, but it also further increases the complexity of the system. In addition, overshoot may make the measuring circuit invalid and damage the electronic equipment. This article proposed a CPT system with a double T-type resonant network and a parameter design method. The proposed system does not generate high over-currents and over-voltages when the pick-up is removed. At the same time, this system can automatically enter standby mode with low power loss when the pick-up is removed, and the system could restore to the normal state condition when the pick-up is moved in. It should be noted that all of the above features can be implemented using the proposed topology without adopting any extra detection and control method, which simplifies the circuit and controller design greatly.

It should be noted that the movement speed of the pick-up depends on the practical applications, the pick-up movement should be fast or slow is decided by the periodic time of the CPT system. To avoid misunderstanding, two statements are defined in this article: the behavior of the pick-up moving slowly is called "move in" and "move out" and the behavior of the pick-up moving quickly is named "switch ON" and "switch OFF."

This article is organized as follows. Section II describes the topology of the proposed CPT system and analyzes the characteristics of T-CLC and T-LCL resonant networks. Section III presents the mathematical models of the system under no-pick-up and normal conditions; the relationships of the resonant network components are derived. Section IV provides the parameter design method of the system. Section V validates the feasibility and validity of the proposed CPT system and its parameter design method with MATLAB simulation and experimental. Finally, Section VI is the conclusion.

II. CPT System With Double T-Type Resonant Network

The proposed CPT topology together with the input inverter and output rectifier is illustrated in Fig. 1. C_{s1} and C_{s2} are the coupling capacitor, the three resonant inductors (L_1, L_2, and L_3), together with the two resonant capacitors (C_1, C_2), form the resonant network of the proposed CPT system. The primary transmitting side is made up of two primary transmitting plates, the resonant network, a full-bridge inverter composed of four power MOSFETs S1–S4, and a dc power source $E_{\rm dc}$. The two

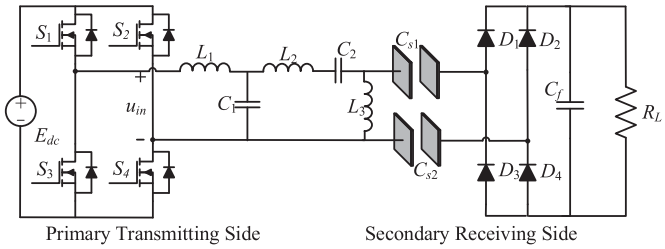

Fig. 1. Schematic for CPT by electric field resonance approach.

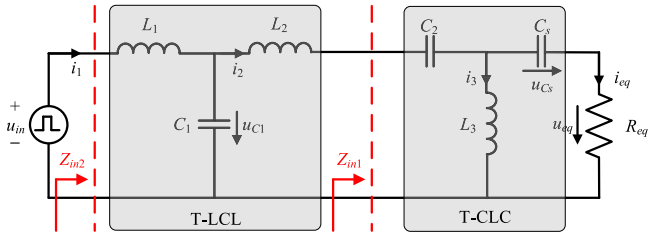

Fig. 2. Equivalent circuit of the proposed CPT.

receiving plates, together with a full-bridge rectifier with diodes D_1, D_2, D_3, and D_4 followed by a resistor R_L are adopted as the secondary receiving side. It should be noted that there is no compensation component on the secondary side of the proposed CPT system, which is helpful to minimize the volume, weight, and cost of the pick-up for a CPT system.

In this article, the cross-coupling capacitance in the coupling structure is much lower than the value of C_{s1} and C_{s2}. For simplicity, the cross-coupling capacitance is ignored, the same way has been adopted in [20]. Thus, the coupling capacitance could be equivalent to two capacitances C_{s1} and C_{s2}.

In Fig. 1, the current is the same on C_{s1} and C_{s2} because it is in series. They are equivalent to one capacitor C_s with the series-connected value of C_{s1} and C_{s2}, the equivalent circuit for Fig. 1 is obtained and shown in Fig. 2. $R_{\rm eq}$ is the effective ac resistance presented by the rectifier and the load, the equivalent ac resistance can be modeled as $R_{\rm eq}= 8R_L/\pi^2$. Assume that all the switches and the input voltage source are ideal, then the output of the inverter is equivalent to a pulse voltage source $u_{\rm in}$. It can be seen from Fig. 2 that L_1, L_2, and C_1 form a T-type *LCL* resonant network while C_2, C_s, and L_3 form a T-type *CLC* resonant network. Therefore, the proposed CPT system has a double T-type resonant network.

The input impedance of the T-*CLC* resonant network can be obtained as

$$Z_{\rm in1} = \frac{1-{\omega_{n1}}^2-{\omega_{n1}}^2/\lambda_1+j\omega_{n1}\left(1-{\omega_{n1}}^2\right)/Q_1}{j\omega_{n1}\omega_{01}C_2\left(1-{\omega_{n1}}^2/\lambda_1+j\omega_{n1}/Q_1\right)} \quad (1)$$

where ω_{01}, ω_{n1}, Q_1, and λ_1 denote the resonant angular frequency, the ratio of angular frequency, load quality factor, and the ratio of capacitors, respectively. And

$$\begin{cases} \omega_{01} = 1/\sqrt{L_3C_2} \\ \omega_{n1} = \omega_1/\omega_{01} \\ Q_1 = 1/(\omega_{01}C_sR_{\rm eq}) \\ \lambda_1 = C_2/C_s \end{cases} \quad (2)$$

where ω_1 is the operating angular frequency of the resonant tank. At the natural oscillation frequency corresponding to $\omega_{n1} = 1$, substituting it into (1) yields

$$Z_{\text{in1}} = \frac{Q_1}{\omega_1 C_2 \lambda_1 + j\omega_1 C_2 Q_1 (1 - \lambda_1)}. \tag{3}$$

When $\lambda_1 = 1$, (3) can be reduced as

$$Z_{\text{in1}} = \frac{Q_1}{\omega_1 C_2} = \frac{1}{(\omega_1 C_2)^2 R_{\text{eq}}}. \tag{4}$$

From (4), it can be seen that the T-*CLC* resonant network operates at zero phase angle and the unity power factor is achieved when the normalized angular frequency ω_{n1} and the ratio of the capacitor λ_1 are equal to one, simultaneously. Besides, the input impedance of the resonant tank is inversely proportional to the load resistance, providing impedance transformation downwards or upwards in terms of the value of R_{eq}.

Similarly, L_1 and C_1 form a resonant circuit at resonant angular frequency ω_{02}, so the input impedance of T-*LCL* resonant network can be obtained as

$$Z_{\text{in2}} = \frac{Z_{\text{in1}} \left(1 - {\omega_{n2}}^2\right) + j\omega_{n2}\omega_{02} L_2 \left(1 - {\omega_{n2}}^2 + \lambda_2\right)}{1 - {\omega_{n2}}^2/\lambda_2 + j{\omega_{n2}}^2/(Q_2\lambda_2)}. \tag{5}$$

Here, λ_2 is designed as the ratio of L_2 to L_1, when $\omega_{n2} = 1$, $\lambda_2 = 1$, (5) can be reduced as

$$Z_{\text{in2}} = \omega_2 L_1 Q_2 = \frac{(\omega_2 L_1)^2}{Z_{\text{in1}}} \tag{6}$$

where Z_{in2}, ω_2, ω_{02}, ω_{n2}, and Q_2 denote the input impedance of the T-*LCL* network, operating angular frequency, resonant angular frequency, the ratio of angular frequency, and load quality factor, respectively.

For the proposed double T-type resonant network, as shown in Fig. 2, the load resistance is equalized as a high impedance (Z_{in1}) transformed by the T-*CLC* resonant network, then Z_{in1} can be equivalent to the low impedance (Z_{in2}) by using T-*LCL*, which is beneficial to improved output power.

III. Modeling and Analysis

To simplify the steady-state analysis, the fundamental harmonic approximation (FHA) method has adopted. Based on the Fourier trigonometric series formula, the output voltage of the full-bridge inverter can be expressed as

$$u_{\text{in}}(t) = \frac{4E_{\text{dc}}}{\pi}\left(\begin{array}{c}\sin\omega t + \frac{1}{3}\sin 3\omega t + \frac{1}{5}\sin 5\omega t \\ + \cdots + \frac{1}{n}\sin n\omega t\end{array}\right) \tag{7}$$

where E_{dc} is the amplitude of the output voltage of the inverter and ω is the operating angular frequency of the proposed CPT system

$$u_{\text{in\_fd}}(t) = \frac{4E_{\text{dc}}}{\pi}\sin(\omega t) \tag{8}$$

where $u_{\text{in\_fd}}$ represents the fundamental component of u_{in}.

A. Steady-State Equivalent Circuit of the System With Pick-up

It is obvious that $\omega_1 = \omega_2 = \omega$ according to the equivalent circuit of the proposed CPT system shown in Fig. 2. Therefore, the steady-state equivalent circuit of the proposed CPT system with load can be simplified as Fig. 3 based on (4). It should be noted that the steady-state equivalent circuit of the CPT system with load is identical whether the pick-up is moved in or switched ON.

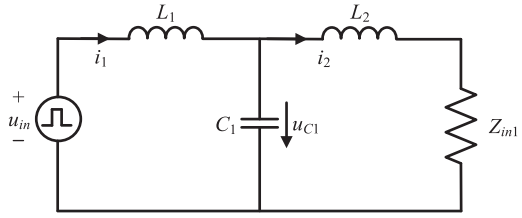

Fig. 3. Steady state equivalent circuit of the proposed CPT system with the pick-up.

Substituting (4) into (6) yields

$$Z_{\text{in2}} = \left({\omega_1}^2 L_1 C_2\right)^2 R_{\text{eq}}. \tag{9}$$

Assuming

$$L_1 = kL_3 \tag{10}$$

where k denotes the ratio of L_1 and L_3. Then, (9) can be expressed as

$$Z_{\text{in2}} = k^2 R_{\text{eq}}. \tag{11}$$

In order to simplify the analysis, the resistance of each element and wire has been ignored in this article. Therefore, the transferred power can be expressed as

$$P = \frac{1}{k^2 R_{\text{eq}}} U_{\text{in}}^2 = \frac{1}{k^2 R_L} E_{\text{dc}}^2. \tag{12}$$

So, the output voltage can be calculated as

$$U_{\text{eq}} = \frac{4}{\sqrt{2}\pi k} E_{\text{dc}}. \tag{13}$$

B. Steady-State Equivalent Circuit of the System With No Pick-Up

When the pick-up is moved out or switched OFF, the steady-state equivalent circuit of the proposed CPT system with no pick-up is shown as Fig. 4. From (2), L_3 resonates with C_2 at ω, thus Fig. 4 can be simplified as the equivalent circuit of Fig. 5.

It can be obtained from (6) that the input impedance of the proposed CPT system approaches infinity after the load is removed or switched OFF

$$Z_{\text{in2}} = R_{\text{inf}} \tag{14}$$

where R_{inf} represents the resistor equals infinity

The proposed CPT system can be transformed to a sinusoidal voltage source in series with a resistor when the pick-up is moved

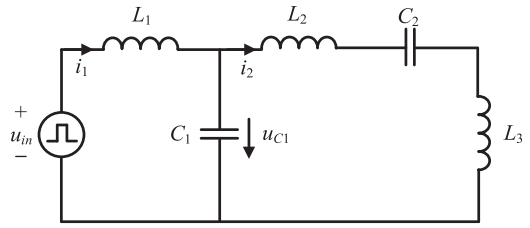

Fig. 4. Steady state equivalent circuit of the proposed CPT system with no pick-up.

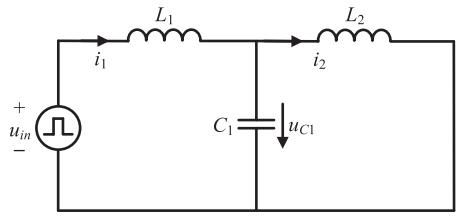

Fig. 5. Simplified equivalent circuit of the proposed CPT system with no pick-up.

in or switched ON and equals to open-circuit when the load is moved out or switched OFF. Therefore, the proposed CPT system could work at a standby state when the pick-up is removed or switched OFF and deliver power when the pick-up is returned to the system without extra additional detection and control circuits.

C. Transient Process During Switching or Moving of the Pick-Up

The proposed CPT system will transit from one steady-state to another when the pick-up is switched ON or switched OFF. The transient response could be analyzed by building the complex frequency domain (Z domain) model. The equivalent circuit of the proposed system in the complex frequency domain when the pick-up is switching OFF is shown in Fig. 6, and the solid line represents a state after switching.

According to the equivalent circuit, the equations can be expressed as (15) as shown at the bottom of next page.

The image function of current and voltage can be derived by (15), then the time-domain solution can be calculated as (16) as shown at the bottom of next page.

Since the system is an alternating circuit in a steady-state, the selection of the initial value will affect the difference of transient response. The maximum amplitude of i_1 is selected as the initial time, where the parameters of the system are shown in Table I listed in Section V. The transient response of i_1 and U_{L3} when the pick-up is switching ON as shown in Fig. 7, the enlarged image is also provided. It can be seen from Fig. 7 that no current spikes are being generated during the pick-up switching process, the small overvoltage has produced when the pick-up is switched OFF, and the overshoot is less than 5%. Meanwhile, the current of i_1 reduces to approximately zero quickly when the pick-up is switched OFF, the switching time is around 0.3 ms.

When the pick-up moving is slow, due to the time scale of a physical movement is significantly larger than the periodic time of the CPT system, the process of the pick-up moving can be

TABLE I
SYSTEM PARAMETERS

Symbol	Parameter	Value
E_{dc}	Input voltage	20V
f	Inverter frequency	495kHz
L_1	Resonant inductor	102.29μH
L_2	Resonant inductor	101.31μH
L_3	Resonant inductor	202.63μH
C_1	Resonant capacitor	1.03nF
C_2	Resonant capacitor	497.3pF
C_s	Coupling capacitance	500pF
R_1	Inductor resistor	0.65Ω
R_2	Inductor resistor	0.62Ω
R_3	Inductor resistor	1.2Ω
R_L	Load resistor	30Ω

equivalent to the variation of the equivalent coupling capacitance C_s. Therefore, when the resistance of each element and wire has been ignored, the current I_1 and voltage U_{L3} can be derived by

$$I_1 = \left| \frac{j\omega C_1 C_s}{kC_2 + kC_s(\omega C_2 R_{\rm eq} - 1)} U_{\rm in} \right|$$

$$U_{L3} = \left| \frac{\omega C_s R_{\rm eq} - j}{k\omega C_s R_{\rm eq} + j(k\omega^2 L_3 C_s - k)} U_{\rm in} \right|. \quad (17)$$

Fig. 8 shows the relationship between the input impedance of the proposed CPT system and the equivalent coupling capacitance C_s, where the parameters of the resonant network are the same as those of Table I listed in Section V. It can be seen from Fig. 8 that the input impedance of the proposed CPT system is minimum when the pick-up is fully coupled, and it approaches infinity when the pick-up is removed, which agree well with the aforementioned analysis. Moreover, the input impedance of the proposed CPT system increases gradually with the decreasing of C_s and is greater than its minimum value. Meanwhile, Fig. 8 also shows that the relationship between current amplitude and coupling capacitance, the current amplitude of i_1 and i_3 increases gradually with the increasing of C_s, there is no over-current with increasing of C_s. Therefore, there is no overshoot or unstable condition that will be generated during the transient process of load moving. It needs to be explained that the transient process of load switching will be analyzed by Fig. 9 that shows the amplitude-frequency curve and phase-frequency curve. Before pick-up is removed, that is, when the value of coupling capacitance is 0. The impedance of the system reaches a minimal value at the working frequency and the phase to be zero, which is beneficial for power transmission. According to Fig. 9 ($C_s = 500$ pF), the input impedance of the resonance network gets the maximum value at the working frequency of the system after the pick-up is removed. At this point, the output current of the inverter is nearly zero, and the system satisfies low standby power loss. In fact, the process of the load removing can be equivalent to the process of C_s decreasing, and the amplitude–frequency curve during the pick-up removing ($C_s = 250$ pF) is also shown in Fig. 9.

D. Selection of k

According to (10), k represents the ratio of L_1 and L_3. Based on (2), Fig. 2 can be transformed into different equivalent circuit

models in terms of the value of k. Fig. 10 is the equivalent circuit of the proposed CPT system when $k < 1$, $k = 1$, and $k > 1$. Thus, the equivalent capacitive–reactance X_{Ceq} and the equivalent inductance–reactance X_{Leq} are given by

$$X_{C_{eq}} = \frac{X_{C_2}}{1-k}, k < 1 \tag{18}$$

$$X_{L_{eq}} = (k-1)\, X_{L_3}, k > 1. \tag{19}$$

It is known from (2) that L_3 resonates with C_s. The effective capacitance of capacitive coupler is in the order of a few hundred picofarad for many CPT systems, and the CPT system generally operates at several hundreds of kilohertz to megahertz. Therefore, the value of L_3 is usually up to hundreds of microhenries [13], [20], [24]. If $k < 1$, then $L_1 < L_3$. It is beneficial to reduce the volume and loss of the inductor, and the power transfer capability of the CPT system is also enhanced. Moreover, L_2 and C_2 in Fig. 2 can be replaced by $C_{\rm eq}$ in Fig. 10, when $k < 1$, both the volume and order of the system are reduced with respect to the original CPT system, and only two compensation inductors are needed, but it should be noted that the waveform of i_2 would be affected by the high-order harmonic when using a $C_{\rm eq}$. When $k > 1$, L_2 and C_2 in Fig. 2 can be replaced by $L_{\rm eq}$. L_2 resonates with C_2 if $k = 1$, L_2 and C_2 can be replaced by a conducting wire (short circuit). In this case, the proposed CPT system is equivalent to the composition of two identical inductors (L_1, L_3) and two identical capacitors (C_1, C_s), and compute of the proposed CPT system is equivalent to the order of fifth ($C_s = C_{s1}C_{s2}/(C_{s1}+C_{s2})$).

Combining Figs. 3 and 10, the proposed CPT system provides impedance transformation downwards or upwards in terms of the value of k. From (12) and (13), the output voltage of the system is independent of the load resistance, thus, the system has the characteristic of constant voltage output, and the voltage gain of k was obtained. The designers can select proper k, according to the condition of load, to produce the desired output power at the specified supply voltage and operating frequency. There is no optimal solution for this case, but a compromise. In most applications, $k \leq 1$ is recommended according to the above analysis. Here, in this article, the value of k is 0.5. Once we have k value, L_1, L_2, and C_2 can be designed based on the k value selection.

IV. Parameter Design Method

In the theoretical analysis, the FHA method is used to established the ac impedance model and analyze circuit topology [5], [10], [20], [23]. But in simulation, the full-bridge inverter is considered, and dc voltage is transformed into a high-frequency square-wave, so higher harmonics are carried into the system, and the system cannot be analyzed by the FHA method. Taking use of total harmonics distortion (THD), that is the percentage of fundamental wave and high-order harmonics to judge whether the output current is a quasi-sine wave or not. Therefore, the filtering performance should be evaluated through the THD of the input current i_1 [7]. Here, THD is defined as

$$\mathrm{THD} = \frac{\sqrt{\sum_{n=3,5,7\ldots}^{\infty} {I_n}^2}}{I_1} \times 100\% \tag{20}$$

where I_1 and I_n represent the rms value of the fundamental component and the odd harmonics of the input current i_1, respectively.

According to the above analysis, a system parameters design procedure for the proposed CPT system is provided as Fig. 11. All the resonant network component's relationships are stated with the system parameters design flow chart. Generally, the initial value of operating frequency f is set based on experience, the value of $E_{\rm dc}$ and the initial value of C_s are specified according to the restrictions of application fields, and the value of R_L is determined by the requirement of the load. The k value of the system is around 0.5. The parameters of the L_1, L_3, and C_2 can be calculated using (10) and (2), L_1 and C_1 form a resonant circuit at angular frequency ω.

$$\begin{cases} I_1(s)(sL_1 + R_1 + \frac{1}{sC_1}) - I_2(s)\frac{1}{sC_1} = U(s) + L_1 i_1(0-) - \frac{u_1(0-)}{s} \\ -I_1(s)\frac{1}{sC_1} + I_2(s)(sL_2 + R_2 + \frac{1}{sC_2} + sL_3 + \frac{1}{sC_1}) = L_2 i_2(0-) - \frac{u_2(0-)}{s} + L_3 i_3(0-) + \frac{u_1(0-)}{s} \end{cases} \tag{15}$$

$$\begin{cases} i_1(t) = \mathcal{L}^{-1}[I_1(s)] \\ \qquad = \mathcal{L}^{-1}\left[\begin{array}{r} ((L_2+L_3)(L_1 i_1(0-)+U_s)C_1C_2s^3 + ((L_1 i_1(0-)+U_s)(R_2+R_3) - (L_2+L_3)U_1(0-))C_1C_2s^2 \\ +((-C_1U_1(0-)(R_2+R_3) + L_1 i_1(0-) + L_2 i_2(0-) + L_3 i_3(0-) + U_s)C_2 + (L_1 i_1(0-)+U_s)C_1)s \\ -C_1U_1(0-) - C_2U_2(0-))/(1 + (L_2+L_3)L_1C_1C_2s^4 + (L_1(R_2+R_3) + (L_2+L_3)R_1)C_1C_2s^3 \\ +(C_1R_1(R_2+R_3) + L_1 + L_2 + L_3)) \end{array}\right] \\ u_{L3}(t) = \mathcal{L}^{-1}[I_2(s)(sL_3+R_3) - L_3 i_2(0-)] \\ \qquad = \mathcal{L}^{-1}\left[\begin{array}{r} ((L_2 i_2(0-) + L_3 i_3(0-))L_1C_1C_2s^3 + (R_1(L_2 i_2(0-) + L_3 i_3(0-)) + \\ L_1(u_1(0-) - u_2(0-)))C_1C_2s^2 + (R_1C_1(u_1(0-) - u_2(0-)) + L_1 i_1(0-) + \\ L_2 i_2(0-) + L_3 i_3(0-) + U_s)C_2s - C_2u_2(0-))/(1 + (L_2+L_3)L_1C_1C_2s^4 + \\ (L_1(R_2+R_3) + (L_2+L_3))C_1C_2R_1s^3 + (C_1C_2R_1R_2 + C_1C_2R_1R_3 + L_1C_1 + \\ L_2C_2 + L_3C_2)s^2 + (C_1R_1 + C_2R_1 + C_2R_2 + C_3R_3)s) \end{array}\right] \end{cases} \tag{16}$$

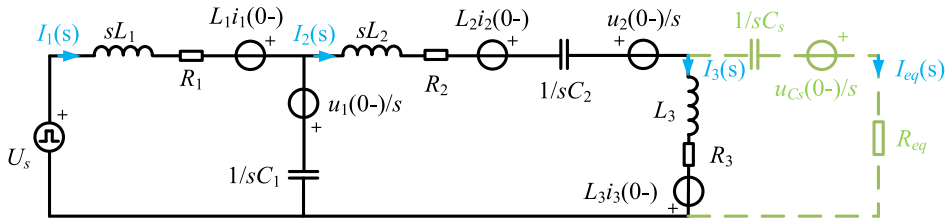

Fig. 6. Equivalent circuit of the proposed system in complex frequency domain when the pick-up is switched OFF.

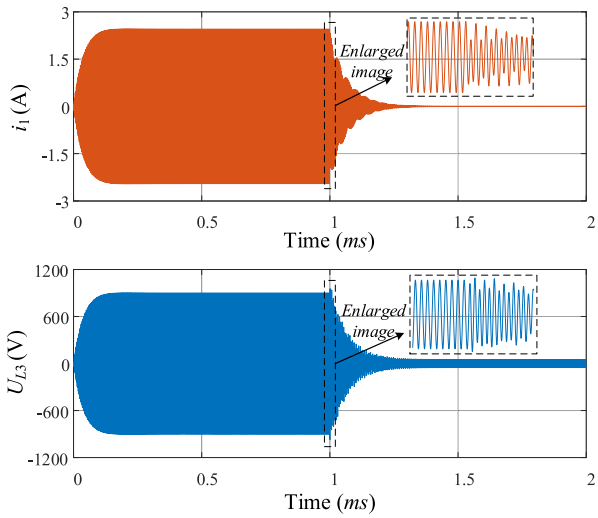

Fig. 7. Transient process of i_1 and U_{L3} when the pick-up is switched OFF.

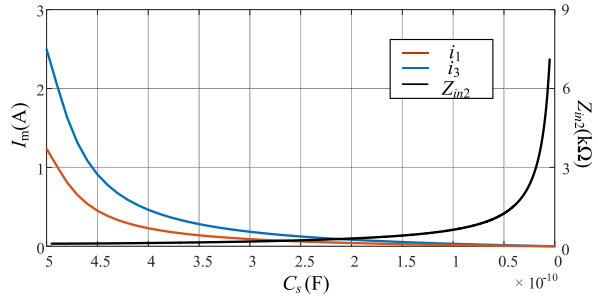

Fig. 8. Input impedance of the CPT system versus C_s and current amplitude I_m.

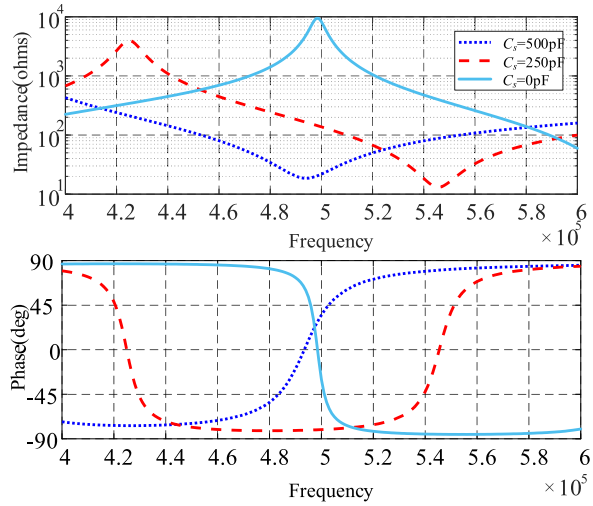

Fig. 9. Relationship between impedance-phase and frequency.

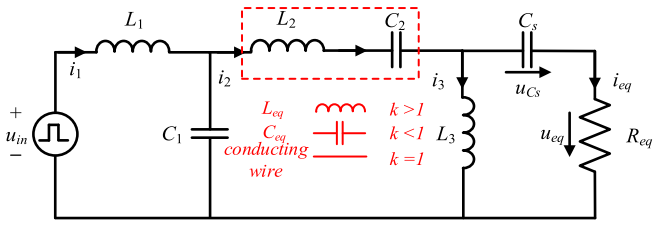

Fig. 10. Equivalent circuit model of the CPT system when $k < 1$, $k = 1$, and $k > 1$.

It should be noted that the THD of the input current i_1 has a marked impact on the power transfer capability of the proposed CPT system, the threshold of the THD should be set as a low value to transfer more power. The system operating frequency f can be adjusted properly if the THD of the input current i_1 is greater than the threshold. The threshold of THD is set below 0.5%, and the initial value of f is set as 500 kHz, reducing frequency properly could obtain the lower THD, so the frequency is selected as 495 kHz.

V. Simulation and Experimental Results

A. Simulation Results

To verify the validity of the proposed CPT system and its parameter design method, the simulation model is built in LT-spice. The R_L value is 30 Ω, the E_{dc} value is 20 V, the k value is 0.5. According to the parameter design method, system parameters for simulations are listed in Table I. Although the inductance is large, the frequency of the system is selected as 495 kHz, which is helpful to reduce electromagnetic interference at a lower frequency, and the volume of the inductor can be reduced by ferrite.

The simulated waveforms of the output voltage and current of the inverter are illustrated in Fig. 12, the THD of the current i_1 is 0.36%. It needs to be emphasized that the inductor L_1 is slightly larger than L_2 to achieve zero voltage switching (ZVS) for the inverter [5], [13], [23]. It can be seen from Fig. 12 that the ZVS operation is achieved because the current lagged the output voltage of the inverter slightly into the resonant tank. The simulation waveforms of i_1 and u_{L3} are similar to the calculated results, as shown in Fig. 7.

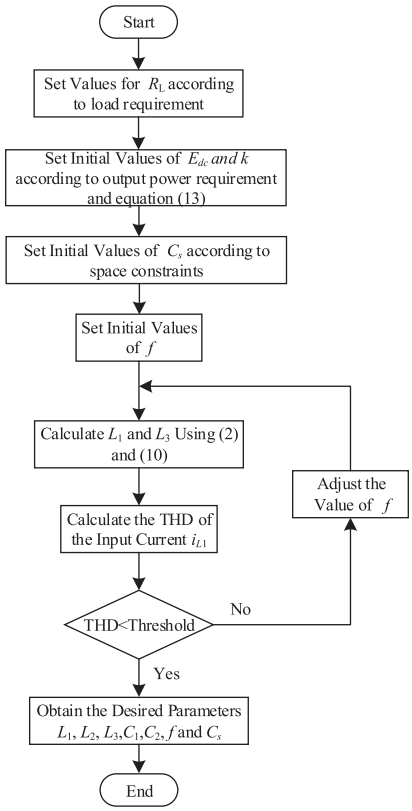

Fig. 11. Flowchart of the system parameters design.

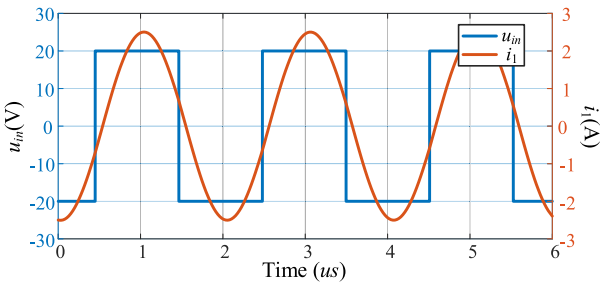

Fig. 12. Simulated waveforms of the output voltage and current of the inverter.

B. Experimental Results

In order to study the practical effect of switching ON and OFF the pick-up, as well as that of pick-up moving. A CPT prototype is built based on the theoretical analysis and simulation research in the previous sections. After verification, experimental results are basically consistent with theoretical analysis, and it is proved that the simplified mode of coupling structure is reasonable. The photograph of the prototype is shown in Fig. 13, the experimental parameters as shown in Table I. To increase the value of coupling capacitance, the coupling plates are tightly coupled, and just separated by the electrical tape, the distance of the two plates is about 0.2 mm. In order to reduce the volume of the inductor, the Litz wire is wrapped around the outside of the blue shell, and the ferrite magnetic cores are placed in the blue shell. The switching devices used in the inverter and rectifier are the STP30NF20 MOSFETs and the HFA08TB60 diodes, respectively.

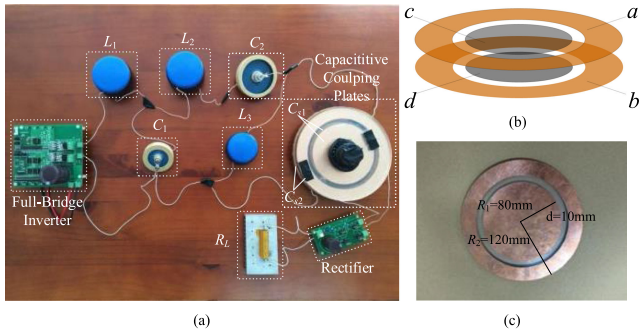

Fig. 13. Prototype of the proposed CPT system.

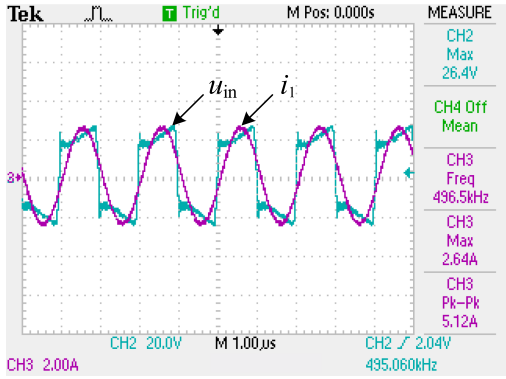

Fig. 14. Experimental waveforms of the u_{in} and i_1 of the inverter.

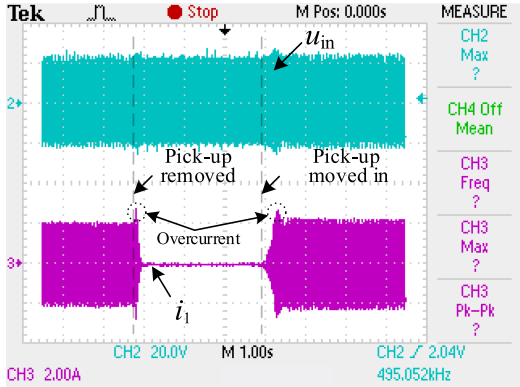

Fig. 15. Experimental transient response of the u_{in} and i_1 when the pick-up move in and move out.

High-frequency ceramic capacitors are used as the resonant capacitors (CCG81-1U/500pF/8kV and CCG81-2U/1000pF/7kV) and the resonant inductors are wound with an air core.

Fig. 14 shows the experimental waveforms of the output voltage and current of the inverter, the input current lags the voltage to achieve zero voltage switching (ZVS), the waveforms are similar to the simulation results shown in Fig. 10. Fig. 15 gives the experimental transient response of the inverter output voltage and current for pick-up moving. The amplitude of the inverter output voltage is almost constant. The current of the inverter reduces approximately tozero (less than 0.01 A) without any current spikes after pick-up is removed, so the input power P_{in} will decrease gradually with the decrease of C_s, and the

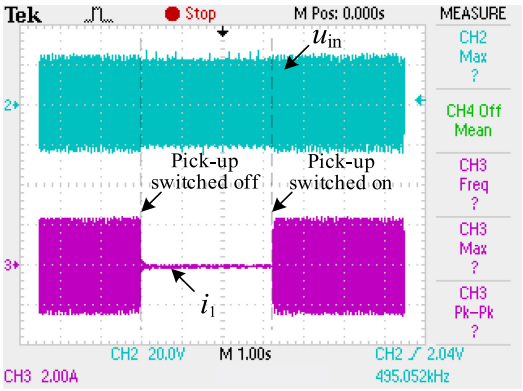

Fig. 16. Experimental transient response of the $u_{\rm in}$ and i_1 when the pick-up is switched OFF and ON.

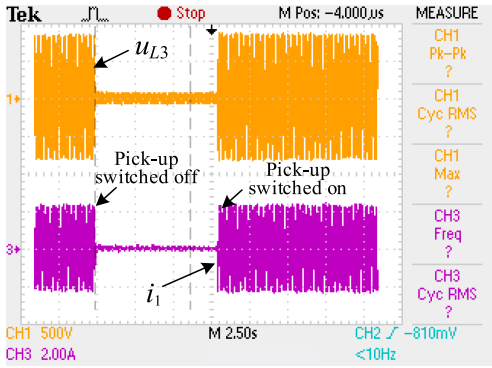

Fig. 17. Experimental transient response of the inductor (L_3) voltage when the pick-up is switched OFF and ON.

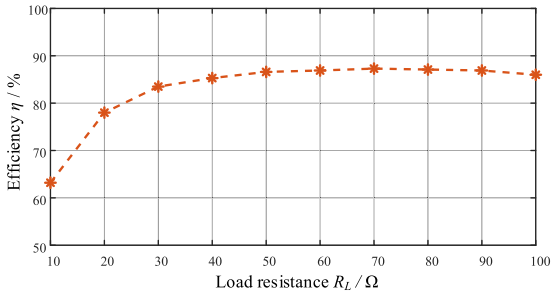

Fig. 18. Curve of load resistance R_L and efficiency η.

current will quickly increase to its rated value after pick-up is moved in. The proposed CPT system operates at the standby state after pick-up is removed, and restores to deliver power after the pick-up is moved in. The semiconductor switches of the inverter are well protected from overcurrent and overvoltage all the time. It should be explained that the physical movement of the load is carried out manually by moving the whole power pick-up with respect to the primary transmitter. The overcurrent of i_1 is caused by the coupling change during the pick-up moving process, thus the experimental results of each operation are slightly different due to the incontinency in the manual movement. In the simulation part, the transition between switch ON and OFF is around 4 ms, it can be observed that the change of switch process more clearly. However, the transition between switch ON and OFF can not be reached in a small time at the experimental conditions.

Fig. 16 shows the experimental transient response of the inverter output voltage and current for load switching. The operation of pick-up switching is achieved by just connecting and disconnecting the load resistor (R_L) by a semiconductor switch at the dc side before the filtering capacitor, the same as removed pick-up. The experimental result of pick-up switching follows the same trends as that of physical load movement, indicating that the proposed CPT system can work well in both situations, and the response time of the pick-up switching is short than physical movement. From Fig. 14, the current of i_1 reduces to approximately zero quickly when the pick-up is switched OFF, the system achieves low standby loss without any control.

Fig. 17 illustrates the experimental transient response of the voltage across the inductor (L_3) for load switching. It can be seen from Fig. 17 that no voltage spikes are being generated during the pick-up switching process. Especially, the voltage across the coupling plates becomes zero after the pick-up is switched OFF.

When the proposed CPT system works in the condition with 30 Ω, the input dc voltage was 20 V and the input dc was measured to be 1.63 A. The dc output voltage was 28.8 V, yielding an output power of 27.4 W. The system efficiency under different load resistance (10–100 Ω) is shown in Fig. 18. The efficiency increases with the increase of the load resistance and then dropped slightly. The system efficiency could be over 84% in the range of 30 to 100 Ω. And the system efficiency decreases when the resistance is less than 30 Ω, which is due to the increase of system loss. The input power is lower than 0.25 W after the pick-up is removed or switched OFF. The proposed CPT system could deliver the required power stably and effectively when the pick-up is coupled or switched ON and work at a standby state after the pick-up is removed or switched OFF without any additional detection and control circuitry. It should be noted that the voltage of C_2 will overshoot when the pick-up is removed, but the amplitude of U_{C2} is far less than the U_{C1} in the work state. The amplitude of U_{C2} is just about 500 V even if the overshoot has occurred, the voltage is still much smaller than the rated voltage and which is within an acceptable range.

According the experiment result, the stress voltage of u_{L3} is about 0.8 kV, therefore, the stress voltage in u_{L3} should be analyzed with the output power. The stress voltage of u_{L3} can be derived by

$$U_{L3m} = \sqrt{2P} \cdot \sqrt{R_{\rm eq} + \frac{\omega^2 {L_1}^2}{k^2 R_{\rm eq}}}. \tag{21}$$

The curve of output power and the stress voltage can be obtained by formula (21), as shown in Fig. 19. The slope of the curve decreases with increasing output power, the stress voltage in u_{L3} is controlled and it will not be over the acceptable range.

The loss distribution of the proposed system is depicted in Fig. 20. The power loss in the compensation inductors, capacitors, MOSFETs, and diodes can be calculated according to [25]. The purpose of the experiment is to validate the characteristic of the topology and correctness of the parameter design method. In the experiment, the efficiency of the system is only 84% due

TABLE II
COMPARISONS WITH OTHER COMPENSATION TOPOLOGIES

Topologies	No.of external components		Efficiency	Transient standby performances		
	Primary-side	Secondary-side		Not high Over-voltage	Not high Over-current	Low standby power losses
LCL-LC [13]	3	2	80%		√	
LCLC-LCLC [20]	4	4	90.7%	√	√	
LC-LC [22]	2	2	74.8%	√	√	
Z-impedance compensation [23]	7	0	83%	√		
This work	**5**	**0**	**84%**	**√**	**√**	**√**

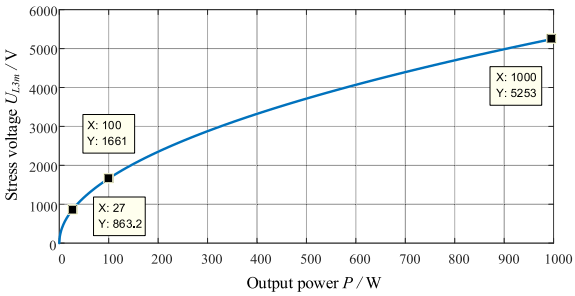

Fig. 19. Output power P versus the stress voltage u_{L3m}.

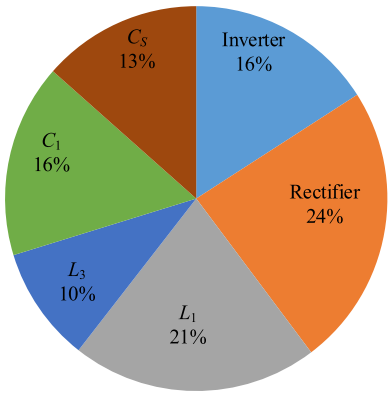

Fig. 20. Power loss distribution of the proposed system components.V.

to the loss of inverter and rectifier is in large proportion, and the high-performance electric device (SiC diode) is not applied in the rectifier, which results in low efficiency. The ratio of losses with L_2 and C_2 is not shown in the figure because the losses are small. Future research will focus on system optimization to minimize losses and increase efficiency.

C. Comparison With Other Compensation Topologies

Many topologies have been proposed in previous studies. The proposed system has been compared with other topologies in the number of external components, efficiency, and transient standby performances, respectively. The comparison results are shown in Table II. In Table II, compared to those usually used topology, the proposed topology has better transient standby performance. And there have no compensation components on the load side, which is helpful to minimize the volume and weight of the load side in practical applications.

VI. CONCLUSION

This rticle proposed a CPT system with a double T-type resonant network for mobile device charging/supply. The equivalent impedance equations were derived when no there is no pick-up and normal condition. The transient process of the system is analyzed. A system parameter design method is presented based on analysis of the T-CLC and T-LCL resonant networks. At last, a CPT system is designed and the analytical results are verified by both simulation and experiment.

The advantages of the proposed CPT system are as follows. First, the circuit components and the semiconductor switches in the inverter of the proposed CPT system are well protected. Second, the system satisfies low standby power losses without extra control circuits when the pick-up is removed or switched OFF, and the system could restore the normal state condition when the pick-up is moved in. Besides, the pick-up in the topology has no compensation component, thus minimizing the volume and weight of the pick-up, which is facilitating the charging or power supply of the mobile device.

ACKNOWLEDGMENT

The authors of this article gratefully acknowledge the support of the China National Center for International Research on Wireless Power Transfer Technology.

REFERENCES

[1] S. Y. R. Hui, W. Zhong, and C. K. Lee, "A critical review of recent progress in mid-range wireless power transfer," *IEEE Trans. Power Electron.*, vol. 29, no. 9, pp. 4500–4511, Sep. 2014.
[2] X. D. Qing, Z. H. Wang, Y. G. Su, Y. M. Zhao, and X. Y. Wu, "Parameter design method with constant output voltage characteristic for bilateral LC-compensated CPT system," *IEEE J. Emerg. Sel. Topics Power Electron.*, vol. 8, no. 3, pp. 2707–2715, Sep. 2020.
[3] A. P. Sample, D. A. Meyer, and J. R. Smith "Analysis, experimental results, and range adaptation of magnetically coupled resonators for wireless power transfer," *IEEE Trans. Ind. Electron.*, vol. 58, no. 2, pp. 544–554, Feb. 2011.
[4] Y. G. Su, S. Y. Xie, A. P. Hu, C. S. Tang, W. Zhou, and L. Huang, "Capacitive power transfer system with a mixed-resonant topology for constant-current multiple-pickup applications," *IEEE Trans. Power Electron.*, vol. 32, no. 11, pp. 8778–8786, Nov. 2017.

[5] S. Q. Li, Z. Liu, H. Zhao, L. Y. Zhu, C. Y. Shuai, and Z. Chen, "Wireless power transfer by electric field resonance and its application in dynamic charging," *IEEE Trans. Ind. Electron.*, vol. 63, no. 10, pp. 6602–6612, Oct. 2016.

[6] Y. Fan, Y. Sun, X. Dai, Z. Zuo, and A. You, "Simultaneous wireless power transfer and full-duplex communication with a single coupling interface," *IEEE Trans. Power Electron.*, vol. 36, no. 6, pp. 6313–6322, 2021.

[7] Y. G. Su, H. Y. Zhang, Z. H. Wang, A. P. Hu, L. Chen, and Y. Sun, "Steady-state load identification method of inductive power transfer system based on switching capacitors," *IEEE Trans. Power Electron.*, vol. 30, no. 11, pp. 6349–6355, Nov. 2015.

[8] C. C. Mi, G. Buja, S. Y. Choi, and C. T. Rim, "Modern advances in wireless power transfer systems for roadway powered electric vehicles," *IEEE Trans. Ind. Electron.*, vol. 63, no. 10, pp. 6533–6545, Oct. 2016.

[9] X. Dai, J. Wu, J. Jiang, R. Gao, and U. K. Madawala, "An energy injection method to improve power transfer capability of bidirectional WPT system with multiple pickups," *IEEE Trans. Power Electron.*, vol. 36, no. 5, pp. 5095–5107, May 2021.

[10] Y. Zhang, Z. Zhao, and K. Chen, "Frequency decrease analysis of resonant wireless power transfer," *IEEE Trans. Power Electron.*, vol. 29, no. 3, pp. 1058–1063, Mar. 2014.

[11] C. Liu, A. P. Hu, B. Wang, and N. C. Nair, "A capacitively coupled contactless matrix charging platform with soft switched transformer control," *IEEE Trans. Ind. Electron.*, vol. 60, no. 1, pp. 249–260, Jan. 2013.

[12] Y. G. Su, W. Zhou, A. P. Hu, C. S. Tang, S. Y. Xie, and Y. Sun, "Full-duplex communication on the shared channel of a capacitively coupled power transfer system," *IEEE Trans. Power Electron.*, vol. 32, no. 4, pp. 3229–3239, Apr. 2017.

[13] M. P. Theodoridis, "Effective capacitive power transfer," *IEEE Trans. Power Electron.*, vol. 27, no. 12, pp. 4906–4913, Dec. 2012.

[14] C. Liu, A. P. Hu, G. A. Covic, and N.-K. C. Nair "Comparative study of CCPT systems with two different inductor tuning positions," *IEEE Trans. Power Electron.*, vol. 27, no. 1, pp. 294–306, Jan. 2012.

[15] B. Luo, T. Long, L. Guo, R. Dai, R. Mai, and Z. He, "Analysis and design of inductive and capacitive hybrid wireless power transfer system for railway application," *IEEE Trans. Ind. Appl.*, vol. 56, no. 3, pp. 3034–3042, May/Jun. 2020.

[16] J. Dai and D. C. Ludois, "Single active switch power electronics for kilowatt scale capacitive power transfer," *IEEE J. Emerg. Sel. Topics Power Electron.*, vol. 3, no. 1, pp. 315–323, Mar. 2015.

[17] W. Zhou, Y. Su, L. Huang, X. Qing, and A. P. Hu, "Wireless power transfer across a metal barrier by combined capacitive and inductive coupling," *IEEE Trans. Ind. Electron.*, vol. 66, no. 5, pp. 4031–4041, May 2019.

[18] R. Sedehi *et al.*, "A wireless power method for deeply implanted biomedical devices via capacitively coupled conductive power transfer," *IEEE Trans. Power Electron.*, vol. 36, no. 2, pp. 1870–1882, Feb. 2021.

[19] K. V. T. Piipponen, R. Sepponen, and P. Eskelinen, "A biosignal instrumentation system using capacitive coupling for power and signal isolation," *IEEE Trans. Biomed. Eng.*, vol. 54, no. 10, pp. 1822–1828, Oct. 2007.

[20] F. Lu, H. Zhang, H. Hofmann, and C. Mi, "A double-sided LCLC-compensated capacitive power transfer system for electric vehicle charging," *IEEE Trans. Power Electron.*, vol. 30, no. 11, pp. 6011–6014, Nov. 2015.

[21] H. Zhang, F. Lu, H. Hofmann, W. G. Liu, and C. Mi, "A four-plate compact capacitive coupler design and LCL-compensated topology for capacitive power transfer in electric vehicle charging application," *IEEE Trans. Power Electron.*, vol. 31, no. 12, pp. 8541–8551, Dec. 2016.

[22] F. Lu, H. Zhang, H. Hofmann, and C. Mi, "A double-sided LC-compensation circuit for loosely coupled capacitive power transfer," *IEEE Trans. Power Electron.*, vol. 33, no. 2, pp. 1633–1643, Feb. 2018.

[23] L. Huang, A. P. Hu, A. Swain, and Y. G. Su, "Z-Impedance compensation for wireless power transfer based on electric field," *IEEE Trans. Power Electron.*, vol. 31, no. 11, pp. 7556–7563, Nov. 2016.

[24] X. Wu, Y. Su, A. P. Hu, X. Qing, and X. Hou, "Multi-objective parameter optimization of a four-plate capacitive power transfer system," *IEEE J. Emerg. Sel. Topics Power Electron.*, vol. 9, no. 2, pp. 2328–2342, Apr. 2021.

[25] B. X. Nguyen *et al.*, "An efficiency optimization scheme for bidirectional inductive power transfer systems," *IEEE Trans. Power Electron.*, vol. 30, no. 11, pp. 6310–6319, Nov. 2015.

Zhe Liu received the B.E. degree in electrical engineering from the Chongqing University of Technology, Chongqing, China, in 2014, and the M.E. degree from the College of Electrical Engineering, Kunming University of Science and Technology, Kunming, China, in 2017. He is currently working toward the Ph.D. degree in control theory and control engineering with the College of Automation, Chongqing University, Chongqing, China.

His research interests include capacitive power transfer and the single capacitive coupled wireless power transfer.

Yu-Gang Su (Member, IEEE) received the B.E. and M.E. degrees in industry automation and the Ph.D. degree in control theory and control engineering from Chongqing University, Chongqing, China, in 1985, 1993, and 2004, respectively.

From 2008 to 2009, he was a Visiting Scholar with the University of Queensland, Brisbane, QLD, Australia. He is currently a Professor with the College of Automation, Chongqing University. His research interests include power electronics, control theory and applications, and wireless power transfer.

Yu-Ming Zhao received the B.E. and Ph.D. degrees from the College of Automation, Chongqing University, Chongqing, China, in 2014 and 2019, respectively.

He is currently with the Chongqing Qianwei Technologies Company Ltd., Chongqing, China. His current research interests include wireless power transfer technology and its application.

Aiguo Patrick Hu (Senior Member, IEEE) graduated with B.E. and M.E. degrees from Xian JiaoTong University, Xi'an, China, in 1985 and 1988, respectively, and the Ph.D. degree from The University of Auckland, Auckland, New Zealand, in 2001.

He was with the National University of Singapore, Singapore, for a semester as an Exchange Postdoc Research Fellow. He is currently a Full Professor with the Department of Electrical and Electronic Engineering, The University of Auckland. He has authored or coauthored more than 200 peer-reviewed journal and conference papers, with about 4500 citations, authored the first monograph on inductive power transfer technology, and contributed four book chapters on wireless power transfer modeling and control, and electrical machines. His research interests include wireless or contactless power transfer systems and application of power electronics in renewable energy systems.

Dr. Hu was the recipient of the University of Auckland VC's Funded Research and Commercialization Medal in April 2017.

Xin Dai (Member, IEEE) received the B.S. degree in industrial automation from Yuzhou University, Chongqing, China, in 2000, and the Ph.D. degree in control theory and control engineering from the School of Automation, Chongqing University, Chongqing, China, in 2006.

In 2012, he was a Visiting Scholar with The University of Auckland, Auckland, New Zealand. He is currently a Professor with the School of Automation, Chongqing University. His current research interests include inductive power transfer technology and nonlinear dynamic behavior analysis of power electronics.